

Understanding how long-term global change affects the intensity and likelihood of extreme weather events is a frontier science challenge. This fourth edition of explaining extreme events of the previous year (2014) from a climate perspective is the most extensive yet with 33 different research groups exploring the causes of 29 different events that occurred in 2014. A number of this year's studies indicate that human-caused climate change greatly increased the likelihood and intensity for extreme heat waves in 2014 over various regions. For other types of extreme events, such as droughts, heavy rains, and winter storms, a climate change influence was found in some instances and not in others. This year's report also included many different types of extreme events. The tropical cyclones that impacted Hawaii were made more likely due to human-caused climate change. Climate change also decreased the Antarctic sea ice extent in 2014 and increased the strength and likelihood of high sea surface temperatures in both the Atlantic and Pacific Oceans. For western U.S. wildfires, no link to the individual events in 2014 could be detected, but the overall probability of western U.S. wildfires has increased due to human impacts on the climate.

Challenges that attribution assessments face include the often limited observational record and inability of models to reproduce some extreme events well. In general, when attribution assessments fail to find anthropogenic signals this alone does not prove anthropogenic climate change did not influence the event. The failure to find a human fingerprint could be due to insufficient data or poor models and not the absence of anthropogenic effects.

This year researchers also considered other human-caused drivers of extreme events beyond the usual radiative drivers. For example, flooding in the Canadian prairies was found to be more likely because of human land-use changes that affect drainage mechanisms. Similarly, the Jakarta floods may have been compounded by land-use change via urban development and associated land subsidence. These types of mechanical factors re-emphasize the various pathways beyond climate change by which human activity can increase regional risk of extreme events.

30. CONTRIBUTORS TO THE RECORD HIGH TEMPERATURES ACROSS AUSTRALIA IN LATE SPRING 2014

PANDORA HOPE, EUN-PA LIM, GUOMIN WANG, HARRY H. HENDON, AND JULIE M. ARBLASTER

The record warm Australian spring of 2014 would likely not have occurred without increases in CO₂ over the last 50 years working in concert with an upper-level wave train.

The Event. Australia experienced in 2014 its highest springtime mean maximum temperature (T_{max}) since records began in 1910. The Australian-mean T_{max} was 2.32°C above the 1961–90 mean, and 0.26°C warmer than the previous record set in 2013 (Bureau of Meteorology 2014). While September was very warm, both October and November had the hottest Australia-average T_{max} on record, with maximum temperatures 2.76°C and 2.18°C above their 1961–90 means, respectively, and the south-east was particularly warm (Fig. 30.1a). Here we focus on the causes of the October–November extreme T_{max} anomaly.

Increasing CO₂. The previous monthly records in October and November were found to be six or seven times more likely in the current modelled climate than in the modelled climate with only natural forcing using the fraction of attributable risk (FAR) method of Lewis et al. (2014). Thus it is highly likely that anthropogenic forcing, especially increasing CO₂, played a role in the extreme heat of this event. While the FAR method is useful, below we describe results using a new method that allows for the influence of increasing CO₂ to be assessed within a coupled seasonal forecast framework.

The Australian Bureau of Meteorology's seasonal forecast model POAMA (Cottrill et al. 2013; Hudson et al. 2013) was used and the design of the forecast sensitivity experiments is described in the online supplemental material. The control forecast was ini-

tialized with observed atmosphere, ocean, and land initial conditions for 2014 and the CO₂ concentration was set to current levels (400 ppm). The extreme heat across Australia was captured well (Fig. 30.1b).

The response of the climate system to enhanced levels of CO₂ occurs on a number of time scales: a rapid adjustment in the atmosphere and longer term warming of the ocean. The immediate atmospheric adjustment is accounted for by re-running the control ensemble, but with CO₂ levels set at 1960 levels (315 ppm). The T_{max} ensemble mean anomaly across Australia from the 400-ppm forecast experiment is warmer compared to the 315-ppm experiment (Fig. 30.1c), but this change is not significant and the ensemble has large spread [compare the red and light blue bars in the probability distribution function (PDF) in Fig. 30.1g]. To assess the impacts of the long-term changes in the ocean due to rising levels of CO₂, a “preCO₂” experiment was conducted. The atmospheric CO₂ was set to 1960 levels and the CO₂ forced component of ocean temperatures and salinity since 1960 (termed oceanCO₂anom, see online supplemental material) was also removed from the initial conditions. Removing oceanCO₂anom from the 2014 ocean initial conditions had a far greater impact on predicted Australian temperatures (Fig. 30.1d) than did changing the atmospheric CO₂ alone. Figure 30.1e represents the contribution to Australian October–November temperatures in 2014 from changing atmospheric CO₂ and the ocean temperature response to the last 50 years of CO₂ change and shows widespread warmth across the continent. Figure 30.1f shows the predicted anomaly if the same initial conditions (i.e., synoptic state of the atmosphere) occurred under 1960 CO₂ levels and associated ocean conditions. Although the warmth was significantly reduced in the preCO₂ experiment (Fig. 30.1f) the predicted conditions in October–November 2014 in the absence of increased

AFFILIATIONS: HOPE, LIM, WANG, AND HENDON—Research and Development Branch, Bureau of Meteorology, Melbourne, Victoria, Australia; ARBLASTER—Research and Development Branch, Bureau of Meteorology, Melbourne, Victoria, Australia, and National Center for Atmospheric Research, Boulder, Colorado

DOI:10.1175/BAMS-D-15-00096.1

A supplement to this article is available online (10.1175/BAMS-D-15-00096.2)

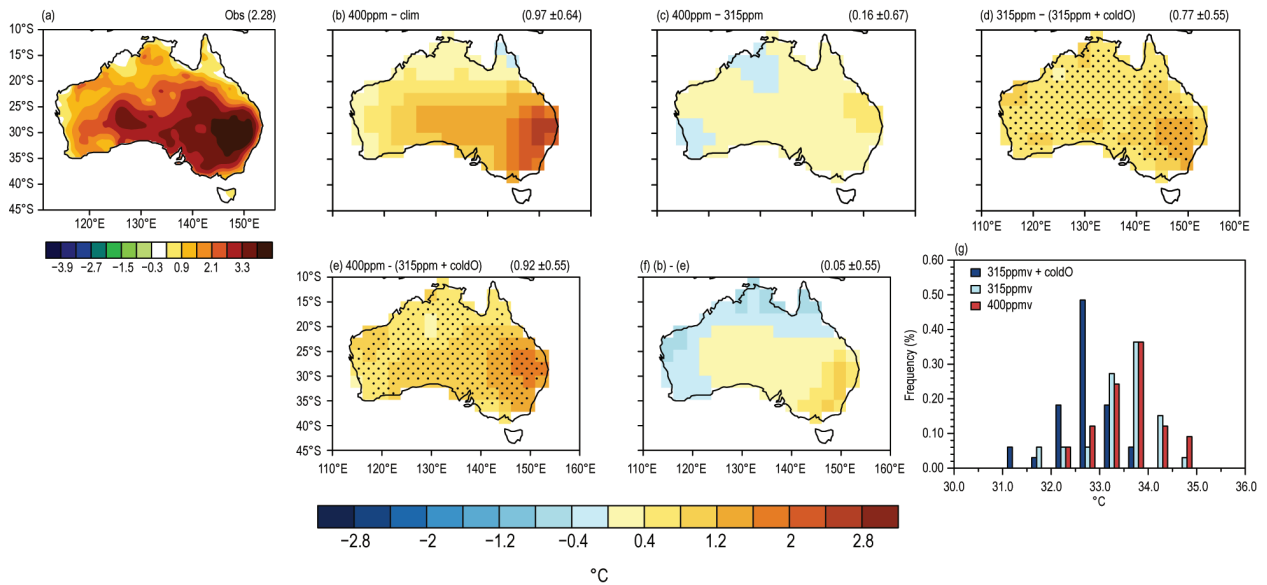


FIG. 30.1. (a) Observed anomaly of Oct–Nov mean Australian Tmax in 2014 relative to 1981–2010 climatology; (b) control forecast Tmax anomaly (with respect to the hindcast climatology) for Oct–Nov, initialized on 21, 25, and 28 September 2014, and with CO₂ levels set at 400 ppm; (c) difference in the forecasts under 400 ppm vs 315 ppm CO₂ concentration; (d) difference in the forecasts made using 2014 realistic initial conditions vs the same conditions but from which oceanCO₂anom is removed under 315 ppm CO₂ (preCO₂); (e) difference between the control forecast (with CO₂ set at 400 ppm) and the forecast with 315 ppm CO₂ and the adjusted ocean initial conditions (oceanCO₂anom removed), which indicates the Tmax associated with increased CO₂ since 1960; (f) difference between (b) and (e), which indicates the Tmax that would have occurred without the influence of increased CO₂ since 1960; (g) PDFs of Australian-average Tmax of 33 ensemble members from the control (400-ppm), 315-ppm, 315-ppm_coldOcean (preCO₂) experiments. The number in parenthesis in the top right corner of (a) is the observed Australian-average Tmax anomaly; in (b)–(f) it is Australian-average Tmax anomaly of the ensemble mean forecast anomaly (or difference between experiments) with an indication of the ensemble spread. Differences with statistical significance greater than 90% confidence level are indicated with stippling. All temperature anomalies in °C.

CO₂ would have still been conducive to a warm event occurring over the far south east of the country.

Compared to the hindcast climatology, forecast Australian late spring temperatures in 2014 were warmer than one standard deviation above the mean in more than half of the control ensemble members (Fig. 30.1g, red bars), but only in 2 of the 33 members from the preCO₂ experiment (Fig. 30.1g, dark blue bars). Given that 2014 was a record event of more than two standard deviations above the mean, no member of the preCO₂ experiment achieved this heat, even while the pattern across Australia reflected anomalously warm conditions in the south-east. Sampling and modelling errors may influence these results. However, the forecast spread of POAMA’s prediction for Australian seasonal Tmax has been shown to encompass the forecast error at short lead times (Hudson et al. 2013) and the clear shift seen in the PDFs between the control and preCO₂ experiments suggest that this result is robust. Other contributors

to the extremity of this event could have arisen from anomalous land conditions in 2014, other large-scale climate drivers, or aspects of the synoptic situation. These are explored below.

Large-scale climate drivers. In order to elucidate the causes of the record heat that worked in concert with increased CO₂, we explicitly describe the contribution from factors known to influence Australian spring temperatures (e.g., Marshall et al. 2013; White et al. 2013) using multiple linear regression (as described in Arblaster et al. 2014). We use three predictors that represent the large-scale climate drivers—ENSO (NINO3.4 index), Indian Ocean dipole (IOD), and the southern annular mode (SAM index)—as well as global mean temperature and antecedent Australian upper level soil moisture. The association of these individual predictors with Australian temperatures is demonstrated here by the regression pattern between Australian Tmax and SST/MSLP (Supplemental Fig.

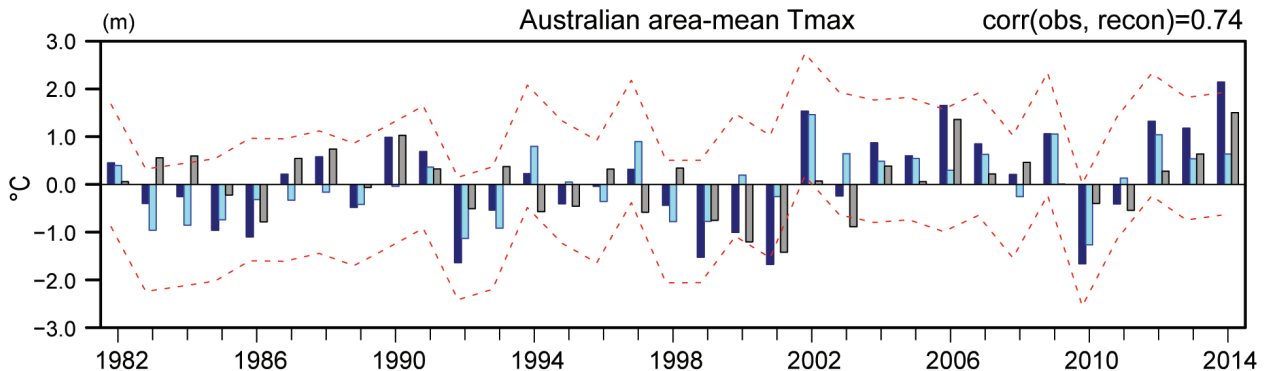
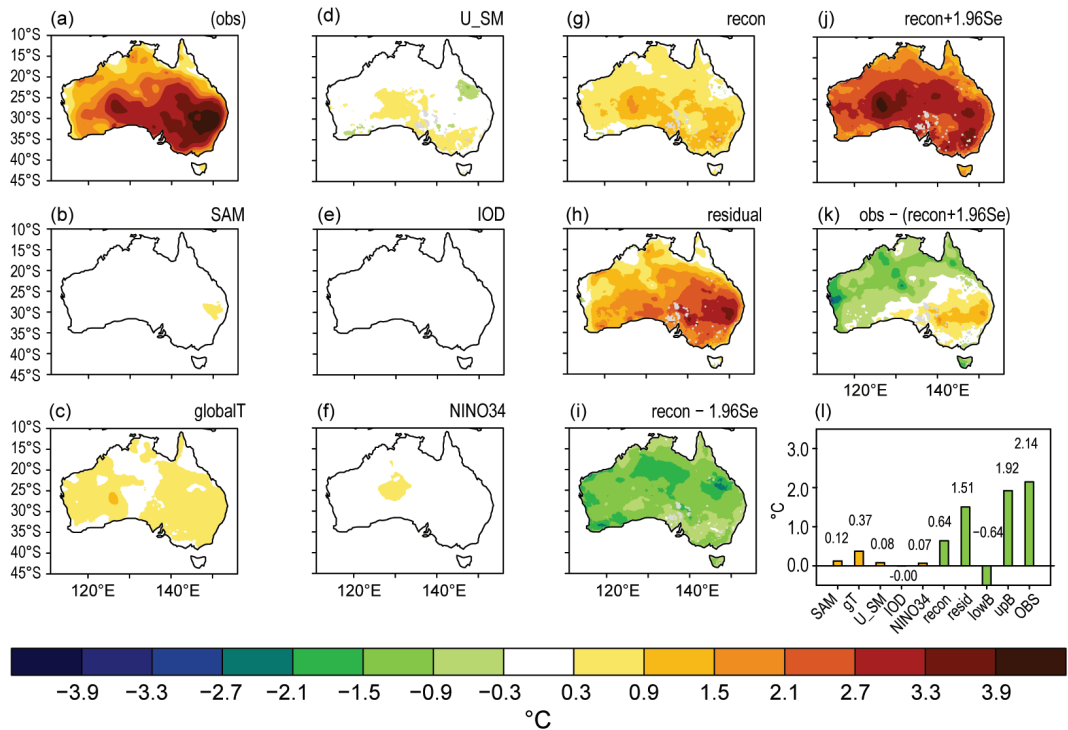


FIG. 30.2. (a)–(l) Patterns of Oct–Nov mean maximum temperature anomaly ($^{\circ}\text{C}$) of 2014 from (a) observations, and the contribution of individual predictors from a multiple linear regression using (b) the southern annular mode, (c) global mean temperature, (d) 2014 September upper-layer soil moisture, (e) the Indian Ocean dipole index, and (f) Niño3.4 SSTs, where each regression map has been multiplied by the size of the predictor in Oct–Nov 2014. (g) The total reconstructed anomaly (sum of panels b–f); (h) the residual, that is, the difference between the observed (a) and reconstructed anomalies (g); (i) the reconstructed anomaly minus the 95% prediction interval; (j) the reconstructed anomaly plus the 95% prediction interval; and (k) difference between (a) and (j). (l) The observed Australian-average maximum temperature anomaly and the contribution by each of the predictors (orange), the total predicted anomaly, the residual, and the predicted anomaly accounting for the 95% prediction interval (green). Anomalies are relative to the 1982–2013 base period. (m) The observed (dark blue), reconstructed (light blue), and residual (gray) Tmax ($^{\circ}\text{C}$) obtained from the multiple linear regression model described in Arblaster et al. (2014) and in the text. Red lines indicate 95% prediction intervals.

S30.3), with signatures of El Niño, positive IOD, and a strong negative SAM associated with warm Australian temperatures.

The observed October–November Australian average Tmax was clearly extreme—it fell outside the bounds of the 95% prediction interval of the regres-

sion model (which accounts for the uncertainty in the strength of the historical relationships Fig. 30.2m). The SST anomaly pattern of late austral spring 2014 (Supplemental Fig. S30.2a) was consistent with weak El Niño, and the tropical Indian Ocean and the far western Pacific Ocean were anomalously warm due

to a warming trend in the last 34 years. However, the regression model reproduces only 30% of the observed warmth across Australia, with global mean temperature being the dominant predictor (Fig. 30.2l). The observed antecedent soil moisture also contributed to the warmth captured by the regression model (Fig. 30.2d), particularly across the south. The pattern of the reconstruction reflects the observed anomalies across the country (Fig. 30.2g), however the magnitude of the 2014 event was much warmer in the east (Fig. 30.2h), and is outside the prediction interval of the regression model (Figs. 30.2j,k). Thus the contribution from large-scale climate drivers such as ENSO, IOD, and SAM as well as antecedent soil moisture to this extreme warm event appears to have been small but positive, and the result of this regression analysis confirms the importance of global mean temperature to this event.

Synoptic situation. While the regression analysis reveals that the large-scale drivers such as ENSO did not contribute strongly to the magnitude of this event, the forecast experiments indicate that there was a predictable contribution to this event over and above the response to global warming (Fig. 30.1f). To explore this further we examine aspects of the observed conditions in October–November 2014. The anomalous circulation at the surface (Supplemental Fig. S30.2b) and in the upper level of the atmosphere (Supplemental Fig. S30.2c) in late austral spring 2014 strongly resemble those typically related to high Tmax over Australia (Supplemental Figs. S30.3c,d). At the surface, an anticyclonic circulation over the Australian continent and cyclonic circulations to its southeast and southwest were evident although they were not part of the SAM in 2014. The upper-level features are characterized by a strong signal of northwest to southeast Rossby wave propagation, which was likely to emanate from the tropical Indian Ocean, positioning high geopotential height anomalies over Australia (e.g., Supplemental Fig. S30.3c).

The degree to which these synoptic conditions are distinct from the large-scale climate drivers was assessed using the reconstruction from the regression model above. Regressing the 200-hPa geopotential height onto the time series of reconstructed Tmax from Fig. 30.2m (Supplemental Fig. S30.4a) does not capture the high geopotential height anomaly described above, while regression onto the residual (Supplemental Fig. S30.4b) highlights the high geopotential height over the country. This suggests that in the upper atmosphere, the synoptic situation of

late spring 2014 was largely uncaptured by the five predictors of the regression model. At the surface, this distinction is less clear, and the regression of MSLP onto the reconstructed Tmax (Supplemental Fig. S30.4c) has some similarity with the regression onto the observed series (Supplemental Fig. S30.3d) while the residual has less. This highlights that this upper-level feature is important in explaining the extremity of this warm event.

Further analysis reveals this Rossby wave train was likely to be promoted by the anomalously high rainfall in the tropical central Indian Ocean (Supplemental Fig. S30.2d). Regression of global 200-hPa geopotential height and rainfall onto the tropical central Indian Ocean rainfall (red box in Supplemental Fig. S30.5a,b) that is independent of IOD, reveals a similar wave train pattern and rainfall anomaly pattern to those of late spring 2014 (Supplemental Fig. S30.5 compared to Supplemental Figs. S30.2c,d). Significant trends in rainfall in this region have been inferred in observations (e.g., Deser and Phillips 2006) over the late 20th century, suggesting a potential trend in this type of synoptic system, but that is a topic for further study.

Conclusions. The record late spring temperatures over Australia in 2014 were analysed using both regression analysis and experiments with a seasonal forecast system. These varied approaches to defining the contributors to the warmth across Australia in late spring 2014 have proved complementary. The impact from ENSO, IOD, and SAM were minor and the antecedent land surface conditions played only a small role, but anomalous Rossby wave train activity was believed to be important to building heat across Australia. The immediate atmospheric adjustment to the changes in CO₂ levels over the last 50 years contributed to the heat, but the major driver of the Australian late spring 2014 heat was the long-term response to CO₂ levels over that time as expressed by an upward trend in oceanic temperature. No members of the preCO₂ experiments achieved the heat of late spring 2014. In summary, each season's warmth will be determined by a combination of anthropogenic forcing and internal variability, in 2014 the enhanced levels of CO₂ likely helped build the heat associated with an anomalous Rossby wave train into a record breaking event.

ACKNOWLEDGMENTS. We thank Matthew Wheeler, Debbie Hudson, David Karoly, Thomas Peterson and two anonymous reviewers for their

constructive comments on this manuscript. This work has been undertaken as part of the Australian Climate Change Science Programme, funded jointly by the Australian Department of the Environment, the Bureau of Meteorology and CSIRO.

REFERENCES

- Arblaster, J. M., E.-P. Lim, H. H. Hendon, B. C. Trewin, M. C. Wheeler, G. Liu, and K. Braganza, 2014: Understanding Australia's hottest September on record [in "Explaining Extremes of 2013 from a Climate Perspective"]. *Bull. Amer. Meteor. Soc.*, **95** (9), S37–S41.
- Bureau of Meteorology, 2014: Special climate statement 50: Australia's warmest spring on record. Bureau of Meteorology, 9 pp. [Available online at www.bom.gov.au/climate/current/statements/scs50.pdf.]
- Cottrill, A., and Coauthors, 2013: Seasonal forecasting in the Pacific using the coupled model POAMA-2. *Wea. Forecasting*, **28**, 668–680, doi:10.1175/WAF-D-12-00072.1.
- Deser, C., and A. S. Phillips, 2006: Simulation of the 1976/1977 climate transition over the North Pacific: Sensitivity to tropical forcing. *J. Climate*, **19**, 6170–6180.
- Hudson, D., A. G. Marshall, Y. Yin, O. Alves, and H. H. Hendon, 2013: Improving intraseasonal prediction with a new ensemble generation strategy. *Mon. Wea. Rev.*, **141**, 4429–4449, doi:10.1175/MWR-D-13-00059.1.
- Lewis, S., D. Karoly, and M. Yu, 2014: Quantitative estimates of anthropogenic contributions to extreme national and state monthly, seasonal and annual average temperatures for Australia. *Aust. Meteor. Oceanogr. J.*, **64**, 215–230.
- Marshall, A. G., D. Hudson, M. Wheeler, O. Alves, H. H. Hendon, M. J. Pook, and J. S. Risbey, 2013: Intra-seasonal drivers of extreme heat over Australia in observations and POAMA-2. *Climate Dyn.*, **43**, 1915–1937, doi:10.1007/s00382-013-2016-1.
- White, C. J., D. Hudson, and O. Alves, 2013: ENSO, the IOD and the intraseasonal prediction of heat extremes across Australia using POAMA-2. *Climate Dyn.*, **43**, 1791–1810, doi:10.1007/s00382-013-2007-2.

Table 34.I. ANTHROPOGENIC INFLUENCE

ON EVENT STRENGTH †

| | INCREASE | DECREASE | NOT FOUND OR UNCERTAIN |
|--------------------------------|--|-----------------------------|---|
| Heat | Australia (Ch. 31) Europe (Ch.13) S. Korea (Ch. 19) | | Australia, Adelaide & Melbourne (Ch. 29) Australia, Brisbane (Ch.28) |
| Cold | | Upper Midwest (Ch.3) | |
| Winter Storms and Snow | | | Eastern U.S. (Ch. 4) N. America (Ch. 6) N. Atlantic (Ch. 7) |
| Heavy Precipitation | Canada** (Ch. 5) | | Jakarta**** (Ch. 26) United Kingdom*** (Ch. 10) New Zealand (Ch. 27) |
| Drought | E. Africa (Ch. 16) E. Africa* (Ch. 17) S. Levant (Ch. 14) | | Middle East and S.W. Asia (Ch. 15) N.E. Asia (Ch. 21) Singapore (Ch. 25) |
| Tropical Cyclones | | | Gonzalo (Ch. 11) W. Pacific (Ch. 24) |
| Wildfires | | | California (Ch. 2) |
| Sea Surface Temperature | W. Tropical & N.E. Pacific (Ch. 20) N.W. Atlantic & N.E. Pacific (Ch. 13) | | |
| Sea Level Pressure | S. Australia (Ch. 32) | | |
| Sea Ice Extent | | | Antarctica (Ch. 33) |

† Papers that did not investigate strength are not listed.

†† Papers that did not investigate likelihood are not listed.

* No influence on the likelihood of low rainfall, but human influences did result in higher temperatures and increased net incoming radiation at the surface over the region most affected by the drought.

** An increase in spring rainfall as well as extensive artificial pond drainage increased the risk of more frequent severe floods from the enhanced rainfall.

*** Evidence for human influence was found for greater risk of UK extreme rainfall during winter 2013/14 with time scales of 10 days

**** The study of Jakarta rainfall event of 2014 found a statistically significant increase in the probability of such rains over the last 115 years, though the study did not establish a cause.

| | ON EVENT LIKELIHOOD †† | | | Total Number of Papers |
|--------------------------------|--|-----------------------------|--|------------------------|
| | INCREASE | DECREASE | NOT FOUND OR UNCERTAIN | |
| Heat | Argentina (Ch. 9) Australia (Ch. 30, Ch. 31) Australia, Adelaide (Ch. 29) Australia, Brisbane (Ch. 28) Europe (Ch. 13) S. Korea (Ch. 19) China (Ch. 22) | | Melbourne, Australia (Ch. 29) | 7 |
| Cold | | Upper Midwest (Ch.3) | | 1 |
| Winter Storms and Snow | Nepal (Ch. 18) | | Eastern U.S. (Ch. 4) N. America (Ch. 6) N. Atlantic (Ch. 7) | 4 |
| Heavy Precipitation | Canada** (Ch. 5) New Zealand (Ch. 27) | | Jakarta**** (Ch. 26) United Kingdom*** (Ch. 10) S. France (Ch. 12) | 5 |
| Drought | E. Africa (Ch. 16) S. Levant (Ch. 14) | | Middle East and S.W. Asia (Ch. 15) E. Africa* (Ch. 17) N.E. Asia (Ch. 21) S. E. Brazil (Ch. 8) Singapore (Ch. 25) | 7 |
| Tropical Cyclones | Hawaii (Ch. 23) | | Gonzalo (Ch. 11) W. Pacific (Ch. 24) | 3 |
| Wildfires | California (Ch. 2) | | | 1 |
| Sea Surface Temperature | W. Tropical & N.E. Pacific (Ch. 20) N.W. Atlantic & N.E. Pacific (Ch. 13) | | | 2 |
| Sea Level Pressure | S. Australia (Ch. 32) | | | 1 |
| Sea Ice Extent | | | Antarctica (Ch. 33) | 1 |
| TOTAL | | | | 32 |

† Papers that did not investigate strength are not listed.

†† Papers that did not investigate likelihood are not listed.

* No influence on the likelihood of low rainfall, but human influences did result in higher temperatures and increased net incoming radiation at the surface over the region most affected by the drought.

** An increase in spring rainfall as well as extensive artificial pond drainage increased the risk of more frequent severe floods from the enhanced rainfall.

*** Evidence for human influence was found for greater risk of UK extreme rainfall during winter 2013/14 with time scales of 10 days

**** The study of Jakarta rainfall event of 2014 found a statistically significant increase in the probability of such rains over the last 115 years, though the study did not establish a cause.